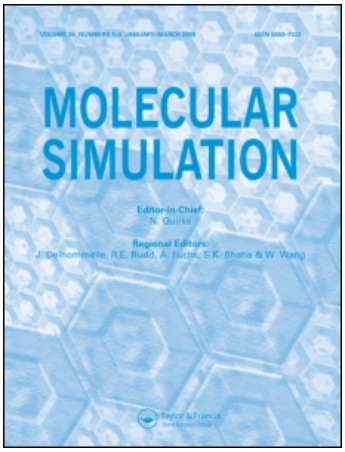


**Molecular Simulation**
Publication details, including instructions for authors and subscription information:
http://www.informaworld.com/smpp/title~content=t713644482

# Size-dependent mobility of platinum cluster on a graphite surface

Jian Chen[ab]; Kwong-Yu Chan[a]
[a] Department of Chemistry, The University of Hong Kong, Hong Kong SAR, China [b] Department of Chemical Engineering, Tsinghua University, Beijing, China

**To cite this Article** Chen, Jian and Chan, Kwong-Yu(2005) 'Size-dependent mobility of platinum cluster on a graphite surface', Molecular Simulation, 31: 6, 527 — 533
**To link to this Article: DOI:** 10.1080/08927020500134292
**URL:** http://dx.doi.org/10.1080/08927020500134292

*Molecular Simulation*, Vol. 31, Nos. 6–7, 15 May – 30 May 2005, 527–533

Taylor & Francis
Taylor & Francis Group

# Size-dependent mobility of platinum cluster on a graphite surface

JIAN CHEN†,‡ and KWONG-YU CHAN*†

†Department of Chemistry, The University of Hong Kong, Pokfulam Road, Hong Kong SAR, China
‡Department of Chemical Engineering, Tsinghua University, Beijing 100084, China

*(Received January 2005; in final form January 2005)*

Molecular dynamics simulations of platinum (Pt) clusters on a graphite surface were performed to study their diffusion and aggregation. The Sutton-Chen many-body potential was used for the Pt–Pt interaction, whereas, a Steele potential was used to calculate the interaction between Pt atoms and carbon (C) atoms of graphite. The results show that at room temperature, the Pt clusters with less than 40 atoms are very mobile with a two-dimensional diffusion coefficient higher than $10^{-11}$m$^2$ s$^{-1}$, but decreasing rapidly with size. The diffusion coefficient of larger cluster has variable size-dependence with local minima at cluster sizes of 50 and 300 Pt atoms and a local maximum at cluster size of 100 atoms. In additional to the overall size of the Pt cluster or nanoparticle, the mismatch between the bottom layer of Pt and graphite also affected the overall Pt–graphite affinity and hence the Pt cluster mobility. The presence of a neighboring Pt cluster can greatly affect mobility. The aggregation of two 50-atom clusters to form a single cluster was observed with the simulation. The relatively stable short dumbbell-like structure of the new cluster resembles previous experimentally observed network of connected Pt nanoparticles on graphite.

*Keywords*: Metallic nanoparticles; Catalyst; Electrocatalysis; Platinum



## 1. Introduction

Metallic nanoparticles is an important class of nanomaterials with diverse applications. Platinum (Pt) is a versatile catalyst, which has been used for many gas-phase and liquid-phase reactions. In heterogeneous catalysis, Pt nanoparticles are normally dispersed and supported on high surface area porous silica or alumina. In electrocatalysis, it is necessary to have the Pt nanoparticles supported on C, which is electronically conducting, in addition to being inert and stable. Important examples of electrocatalytic applications of C supported Pt nanoparticles are found in water treatment and fuel cells [1]. For the high cost of Pt and the best activity of the Pt nanoparticles, it is necessary to keep the nanoparticles dispersed and protected from aggregation in the porous C support. In general, there is a concern of the agglomeration of Pt nanoparticles over time leading to the loss of surface area and activity [2]. Common C supports, like Vulcan 72 have complex structures. Fundamental studies of supported Pt nanoparticles have focused on highly orientated pyrolytic graphite (HOPG) with a well defined planar geometry. The morphology and dynamics of Pt nanoparticles have been studied by scanning tunneling microscopy [3–7] and atomic force microscopy [8–13]. Lee *et al.* [8,9] reported that the Pt cluster size distribution was a function of Pt loading and the average cluster size increased as the Pt loading increased. Clark and Kesmodel [6] studied Pt deposited on HOPG. Very small Pt clusters had the tendency to migrate from one place to another to form a more stable and larger cluster. Lee *et al.* [9] reported that the number of mobile clusters had a maximum around the cluster diameter of 14 nm.

Complementing experimental investigations, molecular dynamics (MD) simulation can probe picosecond time scale dynamics and for smaller length scales of clusters, where experimental studies are difficult. Molecular simulation studies require accurate and computationally convenient interaction potential functions between Pt and C atoms. Relativistic effects of Pt have been of concern [14], but their inclusion in studies of many-atom clusters is computationally prohibitive. A bond-order potential for metal–semiconducator interaction has recently been

*Corresponding author. Fax: + 852-2857-1586. Email: hrsccky@hku.hk

*Molecular Simulation*
ISSN 0892-7022 print/ISSN 1029-0435 online © 2005 Taylor & Francis Ltd
http://www.tandf.co.uk/journals
DOI: 10.1080/08927020500134292

proposed with chemical interaction between Pt–C [15] and C–C atom pairs. C on graphite may not exhibit much semi-conducting behaviour. A combination of physical and chemical adsorption of Pt on HOPG is expected. A simple two-body pair-wise Lennard-Jones (LJ) interaction has been applied for Pt–C simulation [16,17], but fails to capture the many-body interaction and the binding character of decentralized electrons in Pt. A popular and convenient semi-empirical model for Pt has been the Sutton-Chen potential [18] while the Steele potential [19] has been widely used to represent a HOPG surface. Liem and Chan [20] combined the use of the Sutton-Chen potential and the Steele potential by using an effective LJ potential for the Pt–C interaction. This approach of a many body embedded potential for the metal and a pair-wise potential for metal-carbon has also been adopted in a number of simulation studies of Pt on HOPG [21–27] and other metals on HOPG [27–31]. Several simulation studies have investigated the diffusion and mobility of metallic nanocluster on HOPG including gold [27,29–31] and other metals [27]. It is of theoretical and practical interest to study the mobility of Pt clusters on HOPG. In this paper, we report here molecular dynamics simulations of Pt clusters of different sizes on HOPG, with a particular focus on the two-dimensional diffusion behaviour. The aggregation of two clusters into a single cluster was also studied.



## 2. Interaction potentials and simulation details

The simulations were set up as described in previous works [20–23]. The Sutton-Chen potential [18] has been successful in describing the interaction between metal atoms in the bulk solid state. The many-body energy of the $N$-atom cluster is

$$U = \varepsilon_{\mathrm{pp}} \sum_{i=1}^{N} \left[ \frac{1}{2} \sum_{j \neq i}^{N} \left( \frac{\sigma_{\mathrm{pp}}}{r_{ij}} \right)^{n} - c\sqrt{\rho_i} \right] \tag{1}$$

The first term in equation (1) accounts for the repulsion between Pt atomic cores and the second term approximates the bonding energy between these cores due to the surrounding electrons. Since electrons are not explicitly included in the potential function, the local density of atoms, $\rho_i$ with the expression

$$\rho_i = \sum_{j \neq i}^{N} \left( \frac{\sigma_{\mathrm{pp}}}{r_{ij}} \right)^{m} \tag{2}$$

is used to represent the action of electrons.

In equations (1) and (2), $r_{ij}$ is the separation distance between atoms $i$ and $j$, $c$ is a dimensionless parameter, $\varepsilon_{\mathrm{pp}}$ is the energy parameter, $\sigma_{\mathrm{pp}}$ is the lattice parameter of fcc Pt, $m$ and $n$ are positive integers with $n > m$. For Pt, the Sutton-Chen parameters, $c$, $\varepsilon_{\mathrm{pp}}$, $\sigma_{\mathrm{pp}}$, $n$ and $m$ are 34.408, $1.9833 \times 10^{-2}$ eV, 3.92 Å, 10 and 8, respectively [18].

The surface potential proposed by Steele [19] has energy minima representing the adsorption sites and was employed for the interaction between Pt and the HOPG surface. LJ pair-wise interaction was assumed in the Steele potential with the expression

$$U_{\mathrm{Steele}} = E_0(z) + \sum_{i=1}^{5} E_i(z) f_i(s_1, s_2), \tag{3}$$

where $E_0(z)$ and $E_i(z)$ are defined as

$$E_0(z) = \frac{2\pi q \varepsilon_{\mathrm{pc}} \sigma_{\mathrm{pc}}^2}{a_{\mathrm{s}}} \sum_{i=1}^{\infty} \left[ \frac{2}{5} \left( \frac{\sigma_{\mathrm{pc}}}{z + i\Delta z} \right)^{10} - \left( \frac{\sigma_{\mathrm{pc}}}{z + i\Delta z} \right)^{4} \right], \tag{4}$$

and

$$E_i(z) = \frac{2\pi \varepsilon_{\mathrm{pc}} \sigma_{\mathrm{pc}}^6}{a_{\mathrm{s}}} \left[ \frac{\sigma_{\mathrm{pc}}^6}{30} \left( \frac{g_i}{2z} \right)^5 K_5(g_i z) - 2 \left( \frac{g_i}{2z} \right)^2 K_2(g_i z) \right] \tag{5}$$

In the Steele potential expression, $\varepsilon_{\mathrm{pc}}$ and $\sigma_{\mathrm{pc}}$ are LJ parameters of the Pt–C interaction. The LJ parameters $\varepsilon_{\mathrm{pc}}$ and $\sigma_{\mathrm{pc}}$ are obtained by the Lorentz-Berthelot mixing rules, which require the effective LJ parameters of the Pt–Pt interaction. The effective LJ parameters of the Pt–Pt interaction were obtained by a fitting to MD results [20], but the resulting parameters are temperature dependent. At 298 K, the values $\varepsilon_{\mathrm{pp}}^{\mathrm{LJ}}$ and $\sigma_{\mathrm{pp}}^{\mathrm{LJ}}$ are found to be 2336 K and 2.41 Å. The $\sigma_{\mathrm{pp}}^{\mathrm{LJ}}$ parameter in the LJ potential represents the core of the atom, whereas, $\sigma_{\mathrm{pp}}$ in the Sutton-Chen potential represents the crystal lattice. Therefore, they have different values and a small confusion may be caused with the same symbol used conventionally. Since $\sigma_{\mathrm{pp}}^{\mathrm{LJ}}$ is not used in the MD simulations here except to arrive at $\sigma_{\mathrm{pc}}^{\mathrm{LJ}}$, we use $\sigma_{\mathrm{pp}}$ to strictly represent the Sutton-Chen parameter and $\sigma_{\mathrm{pc}}$ to represent the LJ Pt–C parameter. Similarly, $\varepsilon_{\mathrm{pp}}$ is a Sutton-Chen parameter and $\varepsilon_{\mathrm{pc}}$ is a LJ parameter. The corresponding LJ values of $\varepsilon_{\mathrm{pc}}$ and $\sigma_{\mathrm{pc}}$ are 256 K and 2.905 Å, respectively. Details of the Steele potential can be found in [19–21].

The MD simulation was carried out in a three-dimensional cell, which was periodic only along $x$ and $y$ directions. The graphite wall was perpendicular to the $z$-axis and was set to be the lower boundary of the box. The box is rectangular in the $x$ and $y$ dimensions in order to fit the periodic hexagonal graphite lattice. The $x$ and $y$ dimensions were set to be $40 \times 2.46$ and $40 \times 2.13$ Å. The $z$-axis cell height was taken to be 20 $\sigma_{\mathrm{pp}}$ with zero at the midpoint of the axis. The temperature of the system was maintained by *ad hoc* scaling. A timestep of 5 fs was used to integrate the equations of motion in all simulation runs. The annealing method was used to generate the starting configuration of the clusters. First, a face center cubic (FCC) initial configuration of the $N$-atom cluster was created and equilibrated at 2000 K and then the temperature was lowered 100 K for every 1000 time steps. The final configuration was allowed to equilibrate at room temperature with more than 1 million time steps. The configurations thus obtained have a roughly spherical shape with the height less than the diameter. Figure 1

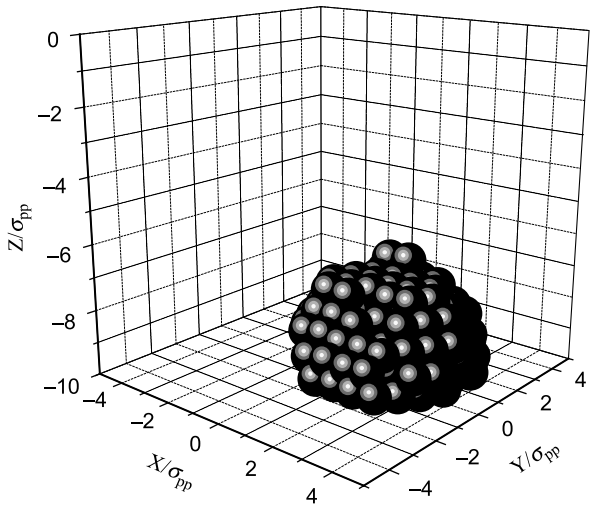


Figure 1. A three-dimensional view of a cluster with 200 Pt atoms on a graphite surface.

shows a typical cluster of 200 Pt atoms after annealing. As discussed in [27], a Pt nanoparticle is more spherical on HOPG compared to a gold nanoparticle, which spreads more on HOPG. This is due to the relative interaction strengths of Pt–Pt and Pt–C. The cutoff in the lateral directions is equal to the dimension of the HOPG surface and minimum image convention was applied in the lateral dimensions. Since there is one cluster in the simulation cell and, inter-cluster interactions only exist between image clusters in neighboring cells. In our simulations, the two-dimensional cluster number density is low and inter-cluster interactions are assumed to be small and negligible. The two dimensional diffusion coefficient of a Pt cluster was calculated by

$$D = \lim_{t\to\infty}\langle \Delta r^2/4t\rangle \tag{6}$$

in which $\Delta r^2 = \Delta x^2 + \Delta y^2$ is the mean lateral square displacement for all Pt atoms or the centre of mass of the cluster. In this work, a period of one million time steps was used in each run for every system. Five consecutive runs were simulated with the input configuration taking from the output configuration of the previous run. The diffusion coefficients of the five runs were averaged to give the final results.

## 3. Results and discussion

### 3.1. Diffusion of clusters on graphite surface

A series of MD simulations were made with one Pt cluster on HOPG. The atom number of the cluster varies from 10, 20, 30, 40, 50, 75, 100, 200, 300, 400 to 500 and the simulations were performed at an equilibrium temperature of 298 K. Figure 2 shows the diffusion coefficient of the Pt cluster as a function of its size in number of atoms. Beyond $N = 30$, the diffusion coefficient is in the order of $10^{-12}\,\mathrm{m^2\,s^{-1}}$. This is in the same order of magnitude as

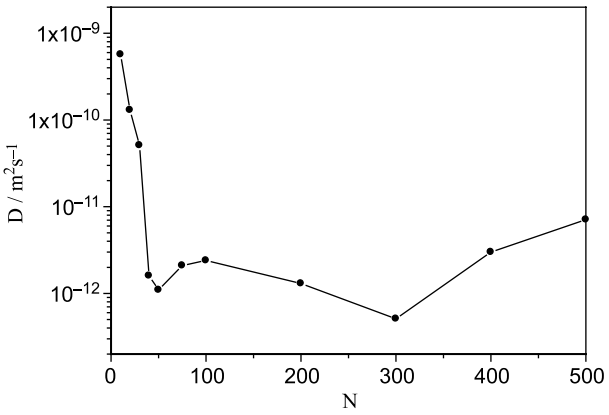


Figure 2. Diffusion coefficient of Pt clusters on the graphite surface.

experimental findings of other metal clusters on HOPG [32]. In figure 2, there are two local minima of diffusion coefficient at cluster size 50 and 300. When the cluster size is $10 \sim 30$, the diffusion coefficient is greater than $5.0 \times 10^{-11}\,\mathrm{m^2\,s^{-1}}$. From the animation of the trajectories of the clusters, much higher mobility can be observed for these smallest clusters, compared to larger clusters simulations. The diffusion coefficient decreases rapidly and monotonically with size until reaching a minimum at cluster size of 50. At sizes between 50 and 500 atoms, there is no clear indication of size dependence and a larger particle can be more mobile. In this range of cluster size, the diffusion coefficient oscillates within an order of magnitude. Due to limitation in computing time, behaviour and size dependence of large clusters $N > 1000$ were not studied.

Factors with opposite effects on mobility appeared to be of dominant importance within different range of cluster sizes. A decrease of mobility with size of the Pt cluster can be explained by a larger inertia and more uncooperative trajectories of atoms preventing motion. The increase of mobility can be attributed to increased misfit of the bottom layer Pt and graphite lattice. Based on some experimental

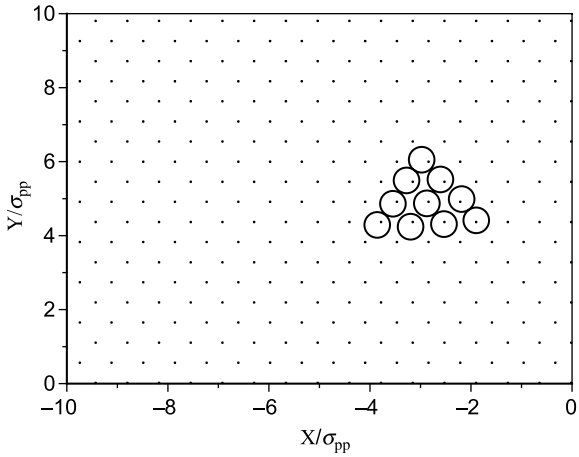


Figure 3. Location of Pt atoms in the lowest layer of the cluster ($N = 30$) compared with the adsorption energy minima (dots) of the graphite surface.

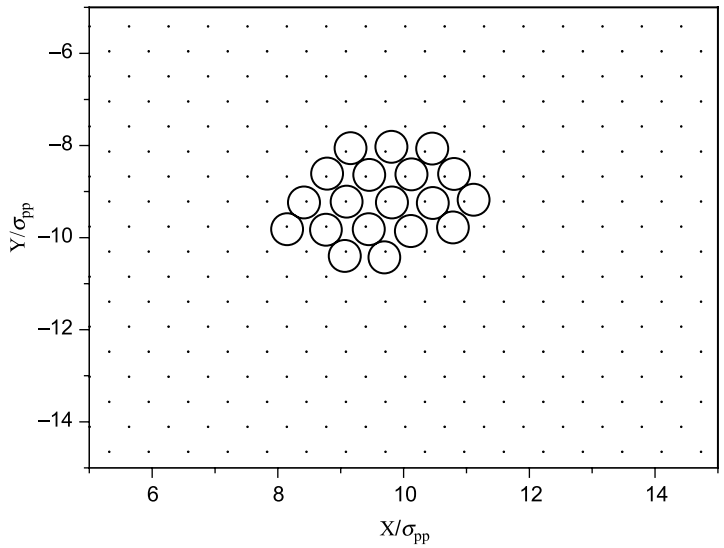


Figure 4. Location of Pt atoms in the lowest layer of the cluster ($N = 50$) compared with the adsorption energy minima (dots) of the graphite surface.



results and simulation studies, Jensen *et al.* [31] commented that the misfit between the gold cluster and graphite substrate was the main parameter determining the diffusion. The commensurability of the bottom layer of the Pt cluster and the graphite lattice shows some dependence on size. The lattice constant of Pt is smaller than that of graphite. While the Pt–Pt interaction is much stronger than that of Pt–C interaction, the cluster maintains its lattice and is physically adsorbed without changing its lattice constant. For a cluster with a small foot area, it is relatively easier to register the bottom Pt atoms with the energy minima of the graphite lattice. For a large cluster, many of the Pt atoms will not fit into the energy minima of the substrate. From figures 3 and 4 for a cluster size of 30 and 50, one can see that the Pt atoms are in good registration with the adsorption sites of the graphite surface. For the Pt cluster with 100 atoms as shown in figure 5, the atoms at the outer rim of the clusters are not in registration with the adsorption sites of the graphite surface. For the Pt cluster with 500 atoms as shown in figure 6, many of the atoms are located at adsorption energy maxima of the graphite lattice. As a result, the average height relative to the graphite lattice, of the bottom layer of the Pt cluster is higher compared to the smaller clusters with better commensurability. The percentage of misfit Pt atoms varies with particle size and is an important factor affecting the mobility of the cluster.

Variable dependence of mobility of Pt nanoparticles on HOPG has been observed by tapping mode atomic force microscopy (AFM) [9]. Maximum mobility was observed for nanoparticles of 10 nm diameter and 1.5 nm height. This result is qualitatively similar to some features of the MD results, except for a different size range. There is a gap in length scale for a direct comparison between simulation and experimental results. The smallest nanoparticle detectable by TMAFM is more than a few nanometers, whereas, thousands of Pt atoms are needed to simulate a 10 nm particle. Interactions between neighbor-

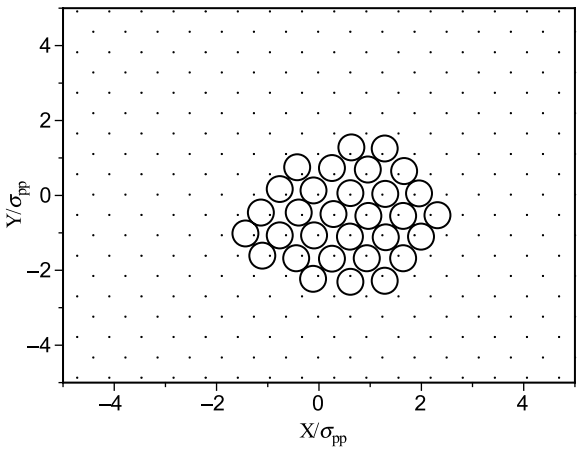


Figure 5. Location of Pt atoms in the lowest layer of the cluster ($N = 100$) compared with the adsorption energy minima (dots) of the graphite surface.

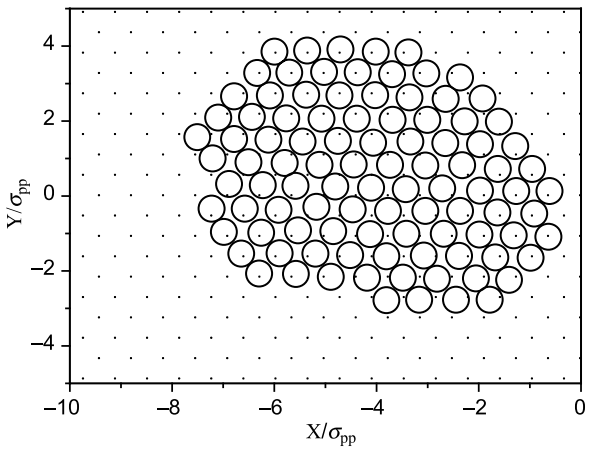


Figure 6. Location of Pt atoms in the lowest layer of the cluster ($N = 500$) compared with the adsorption energy minima (dots) of the graphite surface.

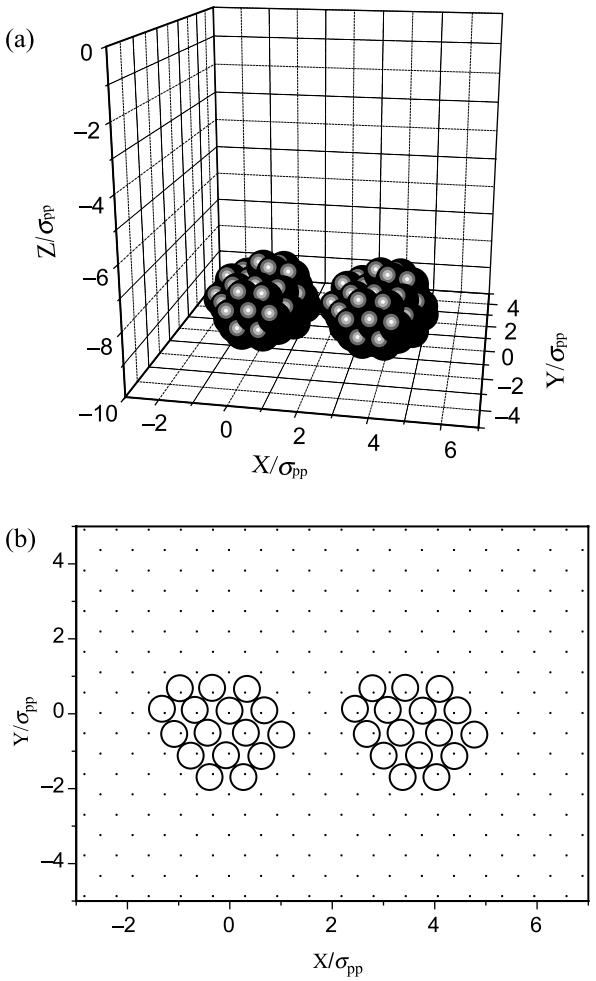


Figure 7. (a) Two clusters with 50 Pt atoms before aggregation ($t = 0.0$ ns). (b) Location of the bottom Pt atoms of the two clusters.

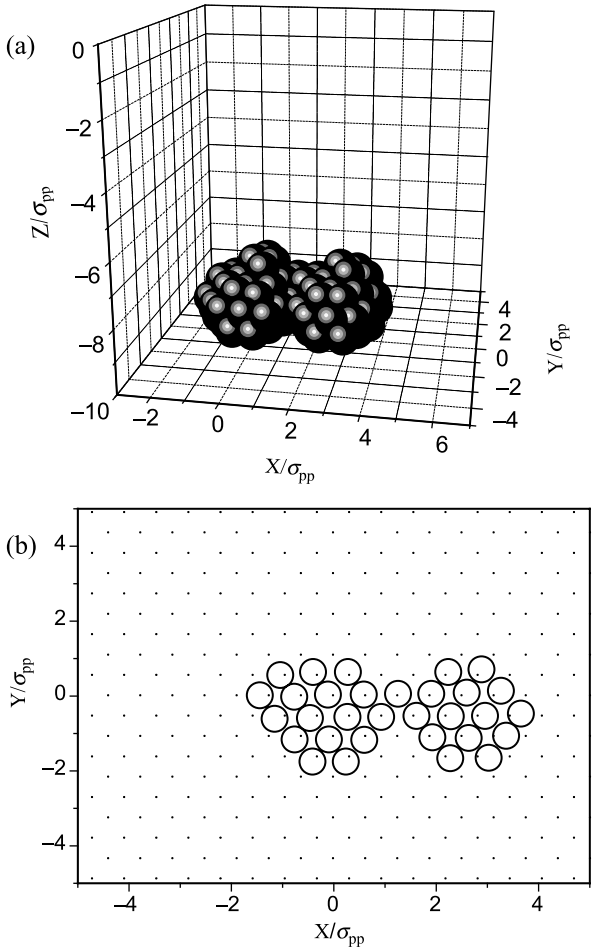


Figure 8. (a) Two clusters with 50 Pt atoms during aggregation ($t = 0.2$ ns). (b) Location of the bottom Pt atoms of the two clusters.

ing Pt nanoparticles will also contribute to the movement in the experiments, whereas, an isolated but adsorbed Pt cluster is simulated here. In ref. [9], there is also the influence of an external force of the AFM tip in the proximity of the Pt nanoparticles. Simulations with the presence of an external force could be made to have a better comparison with the TMAFM results.

In addition to the commensurability of the Pt cluster and the graphite lattices, there are other parameters affecting the lateral diffusion. Since inter-particle forces are absent, the only lateral force present could be due to orientation of the cluster and lateral asymmetry of the atoms within the cluster. These have not been analyzed in our present simulations. The lateral asymmetry will result in an net lateral force between the Pt cluster and the graphite lattice and the orientation will also affect the ease of motion along different directions relative to the basal axes of HOPG.

### *3.2. Aggregation of clusters and its effects on configuration*

To investigate the effect of inter-particle interaction, simulations of a pair of equal size Pt clusters have been performed on the HOPG plane. Pairs of $N = 20$, 50, 100 and 200 Pt clusters have been studied. The two clusters in all pairs attract each other and eventually aggregate to become a single cluster. The aggregation process between two clusters of 50 Pt atoms is reported here. The two identical clusters are put together with a separation distance of $4\sigma_{pp}$. They are attracted towards each other and finally aggregated to become a single cluster. Figure 7(a) and (b) shows the initial configurations and the commensurability of the bottom Pt atoms with the graphite surface. The configuration of first cluster was an equilibrated configuration at 298 K. To generate the second cluster, the $x$ coordinates of the Pt atoms were moved in the $x$ direction for $6 \times 2.46$ Å from the first cluster. In figure 7(b), one can see that identical arrangement of the lowest layer atoms in the two clusters. Figure 8(a) and (b) shows the three-dimensional view and the positions of the bottom atoms after 0.2 ns. The two clusters are in contact with each other, but still retain their own shapes. In figure 7(a), less commensurability can be observed compared to figure 7(b). During the migration, the two clusters not only translate towards each other, but also re-orientate themselves to find the best registration with the graphite surface and the best

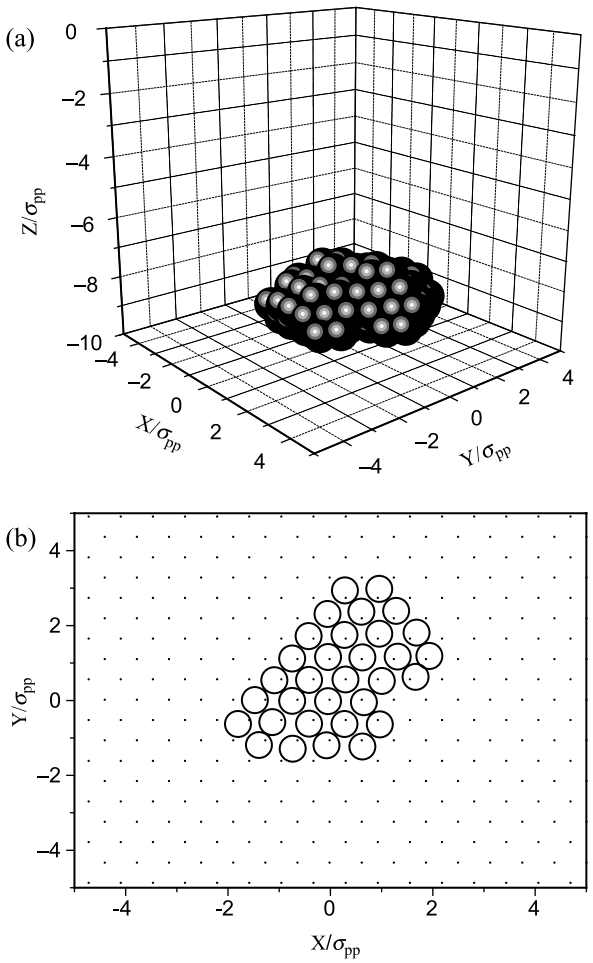


Figure 9. (a) Two clusters with 50 Pt atoms after aggregation ($t = 30.2$ ns). (b) Location of the bottom Pt atoms of the two clusters.

angle to merge with each other. Figure 9a and b shows the configuration after 3.0 ns. The two clusters have aggregated well, but one can tell that it is an aggregation of two clusters with a neck in between. The height of the new cluster is the same as the original height of the two clusters. Figure 9b shows that the lowest layer atoms are in good fit with the adsorption sites. A networked configuration of Pt nanoparticles has been observed on HOPG observed by TMAFM [9]. The two particle connection observed here suggests the possible stability of a networked particle structure, although, the size of the clusters is much smaller than those observed experimentally [9].

## 4. Conclusions

The simulations and results here are insufficient to determine a clear trend of size dependence of the mobility of Pt clusters on HOPG. The results suggest the mismatch of Pt cluster and HOPG lattices to play a critical role. Size-dependence is not a monotone function, as also observed in experiments for a large range of Pt nanoparticles. Pt clusters up to 200 atoms are in general very mobile on HOPG and will aggregate easily. A connected two-particle aggregate with a neck was observed over a period of a few ns, suggesting the possible stability of a networked structure which was also observed in experiments for larger particles.

## Acknowledgements

Funding from Research Grants Council of Hong Kong (HKU 7072/019) is acknowledged.

## References

[1] K.Y. Chan, J. Ding, J. Ren, S.A. Cheng, K.Y. Tsang. Supported mixed metal nanoparticles for fuel cell electrode. *J. Mater. Chem.*, **14**, 505–516 (2004).
[2] A.C.C. Tseung, S.C. Dhara. Loss of surface area by platinum and supported platinum black electrocatalyst. *Electrochimica Acta*, **20**, 681 (1975).
[3] F. Atamny, A. Baiker. Platinum particles supported on carbon: potential and limitations of characterization by STM. *Surf. Interface Anal.*, **27**, 512 (1999).
[4] S. Lee, H. Permana, K.Y.S. Ng. Investigation by scanning tunneling microscopy of the effect of preparative variables on the degree of aggregation of platinum on highly oriented pyrolytic graphite. *J. Vac. Sci. Technol. B*, **10**, 561 (1992).
[5] S. Eppell, G.S. Chottiner, D.A. Scherson, G. Pruett. Scanning tunneling microscopy of platinum deposits on the basal plane of highly oriented pyrolytic graphite. *Langmuir*, **6**, 1316 (1990).
[6] G.W. Clark, L.L. Kesmodel. Ultrahigh vacuum scanning tunneling microscopy studies of platinum on graphite. *J. Vac. Sci. Technol. B*, **11**, 131 (1993).
[7] S. Lee, H. Permana, K.Y.S. Ng. Effects of annealing and gas treatment on the morphology of platinum cluster size on highly oriented pyrolytic graphite by scanning tunneling microscopy. *Catalysis Lett.*, **23**, 281 (1994).
[8] I. Lee, K.-Y. Chan, D.L. Phillips. Growth of electrodeposited platinum nanocrystals studies by atomic force microscopy. *Appl. Surf. Sci.*, **136**, 321 (1998).
[9] I. Lee, K.-Y. Chan, D.L. Phillips. Atomic force microscopy of platinum nanoparticles prepared on HOPG. *Ultramicroscopy*, **75**, 69–76 (1998).
[10] P.K. Shen, N. Chi, K.-Y. Chan, D.L. Phillips. Platinum nanoparticles spontaneously formed on HOPG. *Appl. Surf. Sci.*, **172**, 159–166 (2001).
[11] N. Chi, K.-Y. Chan, D.L. Phillips. Electrocatalytic oxidation of formic acid by Pt/Co nanoparticles. *Catalysis Lett.*, **71**, 21–26 (2001).
[12] I. Lee, K.Y. Chan, D.L. Phillips. Two dimensional dentrites and three dimensional growth of electrodeposited platinum nanoparticles. *Jpn J. Appl. Phys.*, **43**, 767–770 (2004).
[13] J.V. Zoval, J. Lee, S. Goer, R.M. Penner. Electrochemical preparation of platinum nanocrystallites with size selectivity on basal plane oriented graphite surfaces. *J. Phys. Chem. B*, **102**(7), 1166 (1998).
[14] J. Anton, T. Jacob, B. Fricke. Relativistic density functional calculations for $Pt_2$. *Phys. Rev. Letts*, **89**, 213001 (2002).
[15] K. Albe, K. Nordlund, R.S. Averback. Modelling the metal-semiconductor interaction: analytical bond-order potential for platinum-carbon. *Phys. Rev. B*, **65**, 195124 (2002).
[16] S. Liem, K.-Y. Chan, R.F. Savinell. Molecular dynamics simulation of platinum particles between graphite walls. *Mol. Simul.*, **13**, 47–60 (1994).
[17] S. Liem, K.-Y. Chan. Morphology of platinum clusters between graphite walls. *Mol. Simul.*, **14**, 125–136 (1995).
[18] A.P. Sutton, J. Chen. Long-range Finnis-Sinclair potentials. *Philos. Mag. Lett.*, **61**, 139 (1990).
[19] W.A. Steele. Physical interaction of gases with crystalline solids: 1. gas–solid energies and properties of isolated adsorbed atoms. *Surf. Sci.*, **36**, 317 (1973).

[20] S. Liem, K.-Y. Chan. Effective pairwise potential for simulations of absorbed platinum. *Mol. Phys.*, **86**, 939–949 (1995).
[21] S. Liem, K.-Y. Chan. Simulation study of platinum adsorption on graphite using the Sutton-Chen potential. *Surf. Sci.*, **328**, 119–128 (1995).
[22] G. Wu, K.-Y. Chan. Morphology of platinum clusters on graphite at different loadings. *Surf. Sci.*, **365**, 38–52 (1996).
[23] G. Wu, K.-Y. Chan. Molecular simulation of platinum clusters on graphite. *Surf. Rev. Letts*, **4**(5), 855–858 (1997).
[24] G. Wu, K.-Y. Chan. Molecular simulation of oxygen on supported platinum clusters. *J. Electroanal. Chem.*, **450**, 225 (1998).
[25] S.P. Huang, P.B. Balbuena. Platinum nanoclusters on graphite substrates: a molecular dynamics study. *Mol. Phys.*, **100**, 2165 (2002).
[26] E.J. Lamas, P.B. Balbuena. Adsorbate effects on structure and shape of supported nanoclusters: a molecular dynamics study. *J. Phys. Chem. B*, **107**, 11682 (2003).
[27] S.P. Huang, D.S. Mainardi, P.B. Balbuena. Structure and dynamics of graphite-supported bimetallic nanoclusters. *Surf. Sci.*, **545**, 163 (2003).
[28] H. RafiTabar, H. Kamiyama, M. Cross. Molecular dynamics simulation of adsorption of Ag particles on a graphite surface. *Surf. Sci.*, **385**, 187 (1997).
[29] L.J. Lewis, P. Jensen, N. Combe, J.L. Barrat. Diffusion of gold nanoclusters on graphite. *Phys. Rev. B*, **61**, 16084 (2000).
[30] P. Jensen, A. Clement, L.J. Lewis. Diffusion of nanoclusters on non-ideal surfaces. *Physic E*, **21**, 71 (2004).
[31] P. Jensen, A. Clement, L.J. Lewis. Diffusion of nanoclusters. *Comput. Mater. Sci.*, **30**, 137 (2004).
[32] L. Bardotti, P. Jensen, M. Treilleux, A. Hoareau, B. Cabaud. Experimental-observation of fast diffusion of large antimony clusters on graphite surfaces. *Phys. Rev. Lett.*, **74**, 4694 (1995).